# Assessing the effect of model specification and prior sensitivity on Bayesian tests of temporal signal

John H Tay[1], Arthur Kocher[2,3], Sebastian Duchene[1,4,*],

**1** Peter Doherty Institute for Infection and Immunity, Department of Microbiology and Immunology, University of Melbourne, Melbourne, Australia
**2** Transmission, Infection, Diversification and Evolution Group, Max Planck Institute of Geoanthropology, Jena, Germany.
**3** Department of Archaeogenetics, Max Planck Institute for Evolutionary Anthropology, Leipzig, Germany.
**4** Department of Computational Biology, Institut Pasteur, Paris, France

* sduchene@pasteur.fr

## Abstract

Our understanding of the evolution of many microbes has been revolutionised by the molecular clock, a statistical tool to infer evolutionary rates and timescales from analyses of biomolecular sequences. In all molecular clock models, evolutionary rates and times are jointly unidentifiable and 'calibration' information must therefore be used.

For many organisms, sequences sampled at different time points can be employed for such calibration. Before attempting so, it is recommended to verify that the data carry sufficient information for molecular dating, a practice referred to as evaluation of temporal signal. Recently, a fully Bayesian approach, BETS (Bayesian Evaluation of Temporal Signal), was proposed to overcome known limitations of other commonly used techniques such as root-to-tip regression or date randomisation tests. BETS requires the specification of a full Bayesian phylogenetic model, posing several considerations for untangling the impact of model choice on the detection of temporal signal. Here, we aimed to (i) explore the effect of molecular clock model and tree prior specification on the results of BETS and (ii) provide guidelines for improving our confidence in molecular clock estimates.

Using microbial molecular sequence data sets and simulation experiments, we show that the tree prior can have a substantial impact on the accuracy of temporal signal assessment. In particular, highly informative priors that are inconsistent with the data can result in the incorrect detection of temporal signal and this problem is more pronounced when using a strict molecular clock model. In consequence, we recommend (i) using prior sensitivity analyses and prior predictive simulations to determine whether the prior is reasonable and whether the inferences are robust, (ii) including additional information in the form of internal node constraints or informative molecular clock rate distributions when temporal signal is unclear, and (iii) ensuring the the molecular clock model captures rate variation among lineages.

**Keywords:** Molecular clock, temporal signal, Bayesian phylogenetics, microbial evolution.

## Author summary

Our knowledge of when historical and modern pathogens emerged and spread is largely grounded on molecular clock models. The inferences from these models assume that sequence sampling times must have captured a sufficient amount of evolutionary change, which is typically determined using tests of temporal signal, such as BETS. Although BETS is generally effective, here we show that it can incorrectly detect temporal signal if the chosen evolutionary model makes implausible statements about the evolutionary timescale, a situation that is difficult to diagnose, particularly with complex Bayesian models. We demonstrate that this problem is due to a statistical artefact, that we refer to as tree extension and that it can be minimised by conducting careful prior predictive simulations, and by eliciting biologically plausible priors in the model. Overall, our study provides guidelines for improving our statistical confidence in estimates of evolutionary timescales, with key applications for recently emerging pathogens and data sets involving ancient molecular data.


## Introduction

Molecular sequence data have been essential to unravel the evolutionary history of many organisms. The molecular clock is a statistical approach to estimate the date of phylogenetic divergence events based on the hypothesis that molecular evolution, in the form of substitutions, follows an identifiable statistical process. For example, under the earliest and simplest molecular clock model, known as the strict clock, substitutions are assumed to accumulate at a constant rate over time and across lineages [1]. At the other end of the spectrum, relaxed molecular clock models allow every lineage in a phylogenetic tree to display a different evolutionary rate ( [2] and reviewed in [3]).

All molecular clock models have a fundamental limitation; that evolutionary rates and times are jointly unidentifiable. That is, there exist an infinite number of combinations of evolutionary rates and times that are compatible with a given amount of evolutionary divergence [4, 5]. For this reason, external information allowing to constrain some of the parameters of the model must be used, a process known as a molecular clock calibration. The finding that some organisms accumulate substitutions in a measurable timescale prompted the use of sequence sampling times for calibration, a practice known as 'tip calibration' [6, 7]. The latter is particularly useful for microbial organisms for which fossil information cannot be used, or is not available, to constrain internal node dates.

A fundamental requirement for using tip calibration is that the sequenced data were sampled from a measurably evolving population, i.e. that the the interval of time over which the samples were taken captures an appreciable amount of evolutionary change in the studied organism [8]. For rapidly evolving microbes, such as RNA viruses, this might already be achieved by drawing samples over weeks or months. For more slowly evolving microbes sampling over many years or centuries may be needed. Importantly, whole genome sequencing has been a boon for molecular clock analyses of slowly evolving microbes because the resulting data sometimes contain enough information to warrant calibration using sequences collected over a few months or years [9].

There exist several statistical tests to determine whether a sampled population is measurably evolving behaviour, also known as tests of temporal signal. The root-to-tip regression takes a phylogenetic tree for which the branch lengths measure evolutionary distance (i.e. a phylogram) and fits a linear regression of the distance from the root to the tips as a function of their sampling time [7]. The regression slope is a crude estimate of the evolutionary rate, the $x$-intercept is the time to the most recent common ancestor, and the $R^2$ is a measure of clocklike evolution. In general, the root-to-tip

regression is a powerful tool for visual inspection of the data, for example to detect outliers or identify lineages with particularly low or high evolutionary rates [10–13]. However, because the data points are not statistically independent, resulting statistics such as $p$-values are invalid and cannot be used as formal statistical tests of temporal signal [14]. A different approach, known as the 'date randomisation test', consist of fitting a molecular clock to the data after permuting the sampling times multiple times to obtain a 'null' distribution of the evolutionary rate [15]. The data are considered to have temporal signal if the evolutionary rate estimated with the correct sampling times falls outside such 'null' distribution [15, 16].

In order to overcome the issues associated with the above-mentioned techniques, a fully Bayesian Evaluation of Temporal Signal (BETS) approach was recently proposed [17]. The premise of this test is that the data sampled from a measurably evolving population should have higher statistical fit when the sampling times are included than when they are not, which can be assessed through model selection. In practice, the data are analysed with their correct sampling times (i.e. heterochronous) and with all samples assigned the same date (i.e. isochronous, with the sampling time set to the present), while keeping the rest of the phylogenetic model the same, including the molecular clock, tree prior and substitution model. The log marginal likelihood is calculated in each case to compute log Bayes factors, which quantify the amount of evidence for one model over another, here that with sampling times vs that without. A major advantage of BETS is that it can consider the full model and it naturally accommodates important sources of uncertainty, including that due to radio carbon dating of ancient DNA studies [18].

Most parameters of the phylogenetic model have individual prior probability distributions that can be chosen by the user, for example, the evolutionary rate, or the transition-to-transversion ratio of the HKY substitution model. The prior for the phylogenetic tree topology and branch lengths is usually a branching model, such as a coalescent or birth-death process, which implicitly impose a prior probability distribution on the ages of nodes, and therefore may inadvertently convey highly informative calibration priors. Moreover, model selection, as used for BETS, can be sensitive to the choice of prior, even if the posterior is not [19, 20]. Here we investigate the impact of the tree prior and associated parameters, and the molecular clock model in the detection of temporal signal. We also explore alternative parameterisations of the full Bayesian model that can improve the accuracy of tests of temporal signal.

# Results

## Empirical data analyses

We first explored the effect of model specification on the results of BETS using empirical datasets for which temporal signal was previously detected using other methods. The following three data sets were used: *Vibrio cholerae* [21], the bacterium responsible for cholera; *Powassan virus (POWV)* [22], a tick-borne virus; and *Treponema pallidum* [23], the bacterium that causes syphilis. The *V. cholerae* and *T. pallidum* data sets include ancient samples, and the phylogenetic trees from the POWV and *T. pallidum* indicate complex population structure that is typical of data sets from multiple outbreaks.

We conducted BETS analyses under a coalescent tree prior with constant population size and two possible clock models; a strict and an uncorrelated relaxed clock with an underlying log-normal distribution [2]. Our choice the constant-size coalescent tree prior is based on statistical convenience, as it is fully parametric, but it does is not necessarily an accurate representation of the the biological process. We set up our analyses in BEAST1.10 [24] and calculated log marginal likelihoods with and without sampling

times for each combination of molecular clock model and tree prior (for a tutorial of using BETS see: `https://beast.community/bets_tutorial`).

To assess the impact of the tree prior we considered different prior distributions for the effective population size, $\theta$, the only parameter in the constant-size coalescent. In the exponential-size coalescent, which we also considered in our simulations (see below), this parameter is known as the 'scaled population size' (denoted with the Greek letter $\Phi$) and it is proportional to the population size at present [25]. Both, $\theta$ and $\Phi$ are referred to as a *scale parameters* for time because large values imply more dispersion (the molecular clock rate is also a scale parameter), and they are typically assigned a $1/x$ prior distribution, which is the Jeffrey's prior that is uninformative and invariant to reparameterisation [26]. The $1/x$ prior has attractive attributes because it maximises the signal from the data, but it is an improper distribution (it does not integrate to one over its domain, because $\int_0^\infty \frac{1}{x}$ is undefined), a problem for model comparison using Bayes factors, because marginal likelihood calculations require that all priors be proper distributions [27, 28]. Instead, we selected three prior distributions, an exponential, $\Gamma$ (Gamma), and log-normal, that have been used in recent literature as shown in Table 1.

Our rationale for using different prior distributions on $\theta$ is its impact on parameters that pertain to the molecular clock. In particular, under the coalescent process, the expected time of divergence between sampled lineages is inversely proportional to the population size, meaning that large values of $\theta$ will result in an older time to the most recent common ancestor than small values for this parameter. The prior on $\theta$ will also have an impact on the evolutionary rate for two key reasons. First, by impacting the overall age of the tree, it impacts the length of time over which the sequence data evolved. Second, the default prior for the evolutionary rate in BEAST1.10 is a $\Gamma$ distribution with shape ($\alpha$) of 0.5 and beta ($\beta$, also known as the 'rate') equal to the tree length (sum of all branch lengths) [29, 30]. In this software, this prior is known as the CTMC-rate reference prior and its mean value is 0.5/tree length [30], meaning that it is indirectly impacted by $\theta$ (or $\Phi$).

**Table 1.** Prior distributions for the effective population size of the constant-size coalescent (known as $\theta$ in the constant-size coalescent and different to the scale parameter of the $\Gamma$ distribution).

| Probability distribution function | Parameters |
|---|---|
| Exponential | mean, $\mu = 1.0$ |
| Log-normal | mean, $\mu = 1.0$; standard deviation $\sigma = 5.0$ |
| $\Gamma$ (Gamma) | shape, $\kappa = 0.001$; scale, $\theta = 1000$ |

The *V. cholerae* data set displayed overwhelming support for temporal signal (Table 2 and Fig 1), regardless of the molecular clock model and prior on $\theta$, with log Bayes factors of over 200. Note that a log Bayes factor of 3.2 corresponds to a model posterior probability $\approx$0.95 [31], and is considered as 'very strong support', following Kass and Raftery [32]. Although in this data set the prior on $\theta$ did not impact model selection for detecting temporal signal, it did impact the magnitude of the Bayes factors.

For our other two data sets the impact of the prior on model selection was evident. For *Poawassan virus* the $\Gamma$ and log-normal priors on $\theta$ suggested strong temporal signal, whereas the exponential prior strongly favoured the exclusion of sampling times, according to the strict and relaxed molecular clock models. In our analyses of the *T. pallidum* data set we found support for temporal signal under the strict molecular clock, according to all priors on $\theta$, although with very strong evidence only for the exponential prior and 'positive evidence' for the $\Gamma$ and log-normal priors. Under the relaxed molecular clock model all priors had very strong support against temporal signal.

**Table 2.** Log Bayes factors between isochronous and heterochronous models for each dataset, separated by prior on effective population size, $\theta$

| **Species; Clock Model** | Exponential | Gamma | Log-normal |
|---|---|---|---|
| *Vibrio cholerae*; *Strict Clock* | 355.18 | 379.63 | 382.10 |
| *Vibrio cholerae*; *Relaxed Clock* | 208.97 | 439.63 | 219.60 |
| *Powassan virus (POWV)*; *Strict Clock* | -80.63 | 32.67 | 50.29 |
| *Powassan virus (POWV)*; *Relaxed Clock* | -221.94 | 18.79 | 27.23 |
| *Treponema pallidum*; *Strict Clock* | 105.80 | 2.17 | 1.85 |
| *Treponema pallidum*; *Relaxed Clock* | -34.37 | -1474.14 | -34.04 |

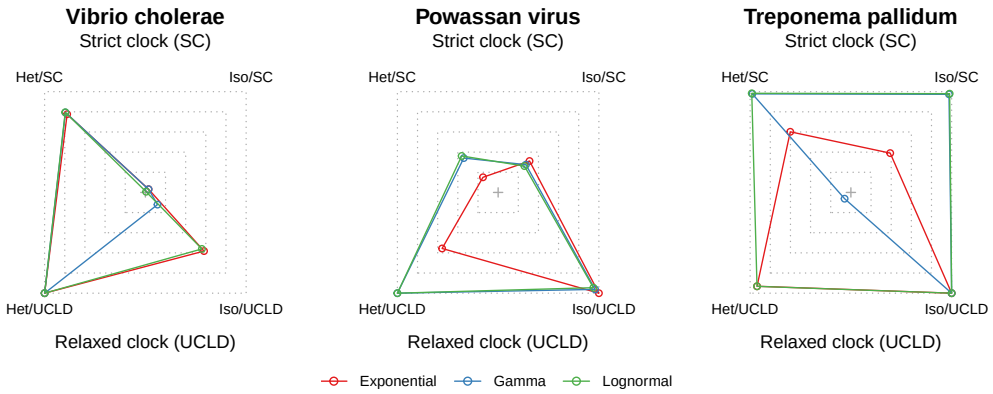


**Fig 1. Relative log marginal likelihoods of empirical data sets**. The polygons represent the relative log marginal likelihoods of each microbe dataset under a different effective population size ($\theta$) prior, analysed with four different configurations. Het (heterochronous) includes sampling, while iso (isochronous) does not include any sampling times. SC is strict clock and UCLD is the uncorrelated lognormal relaxed clock. Red represents an exponential prior on the effective population size, blue is a $\Gamma$ prior, and green is a log-normal prior.

Our empirical data analyses overall demonstrate that the choice of prior has substantial impact on Bayesian model selection and support. In the case of the *V. cholerae* data, the detection of temporal signal was relatively robust to the prior. Consistently, we found that the posterior distribution of key parameters such as the evolutionary rate was not overly sensitive to the prior for this data set (Supplementary material). Moreover, this data set has been shown to have clear clocklike behaviour in root-to-tip regressions and date randomisation tests [33]. In contrast, for the data sets of *Powassan virus* and *T. pallidum*, where temporal signal was not supported for all model configurations, we found that the posterior was more sensitive to the choice of prior (Supporting information).

## Simulation experiments

To understand the impact of the prior on BETS results in more detail, we conducted a set of simulation experiments where the data generating process was well understood. We conducted simulations under four possible conditions: a strict or relaxed molecular

clock model, and where the phylogenetic time-trees were heterochronous or isochronous. Data from heterochronous trees are sampled from a measurably evolving population and are expected to display temporal signal, whereas those from isochronous trees by definition represent non measurably evolving (the time-trees are ultrametric) and should not display temporal signal.

For data generated under heterochronous time-trees, we found that ten out of ten simulation replicates were correctly classified as having temporal signal, using a log Bayes factor of at least 3.2 (Table 3 and Fig 2). This perfect classification, which can be considered a low type II error (where a type II error is failing to support temporal signal when it is truly present), was supported regardless of the prior on $\theta$ and the molecular clock model.

**Table 3. Correctly classified simulation replicates under heterochronous trees.** A total of ten simulations were generated in each case, under heterochronous trees, such that they are expected to display temporal signal. A number of ten represents perfect classification according to the Bayesian evaluation of temporal signal, BETS and a log Bayes factor of at least 3.2 (strong evidence for temporal signal). The rows correspond to three possible priors on the effective population size of the constant-size coalescent, $\theta$. The 'Best clock model' is a situation where we consider the best heterochronous and isochronous model, take their log Bayes factor, and determine temporal signal if it is at least 3.2.

| **True clock model; clock model in analysis** | Exponential | Γ | Log-normal |
|---|---|---|---|
| Strict clock; Strict clock | 10 | 10 | 10 |
| Strict clock; Relaxed clock | 10 | 10 | 10 |
| Strict clock; Best clock model | 10 | 10 | 10 |
| Relaxed clock; Strict clock | 10 | 10 | 10 |
| Relaxed clock; Relaxed clock | 10 | 10 | 10 |
| Relaxed clock; Best clock model | 10 | 10 | 10 |

For our data generated under isochronous trees (with no temporal signal) we found perfect classification under the exponential prior on $\theta$ under both clock models (Table 4 and Fig 3). For most analyses under the Γ and log-normal priors on $\theta$ we found that BETS incorrectly supported the presence of temporal signal, implying a high type I error (the incorrect detection of temporal signal). The exceptions were for analyses of data analysed under a relaxed molecular clock model, regardless of the molecular clock model used for simulation.

A perplexing result occurs under the best molecular clock model for the Γ and log-normal priors on $\theta$. Here we take the log Bayes factor of the best heterochronous model vs the best isochronous model, which produced an increase in the classification error, relative to using the relaxed clock only. This phenomenon likely occurs because the incorrect inclusion of sampling times can mislead molecular clock model selection. As a case in point, one of the simulation replicates under a relaxed molecular clock and an isochronous tree (with no temporal signal) had the following log marginal likelihoods; -4109.87 for the heterochronous analyses with a strict clock, -4117.06 for the isochronous analyses with a strict clock, -4124.35 for the heterochronous analyses with a relaxed clock, and -4118.29 for the isochronous analyses with a relaxed clock. The log Bayes factors under the relaxed clock have strong evidence against temporal signal (log Bayes factor=-6.06 for heterochronous vs isochronous), whereas the opposite is true for the strict clock (log Bayes factor=7.19). However, the best heterochronous model has substantially stronger support than the best isochronous model (here the strict or relaxed molecular clock, whose log marginal likelihoods differ by only 1.3 units). It is

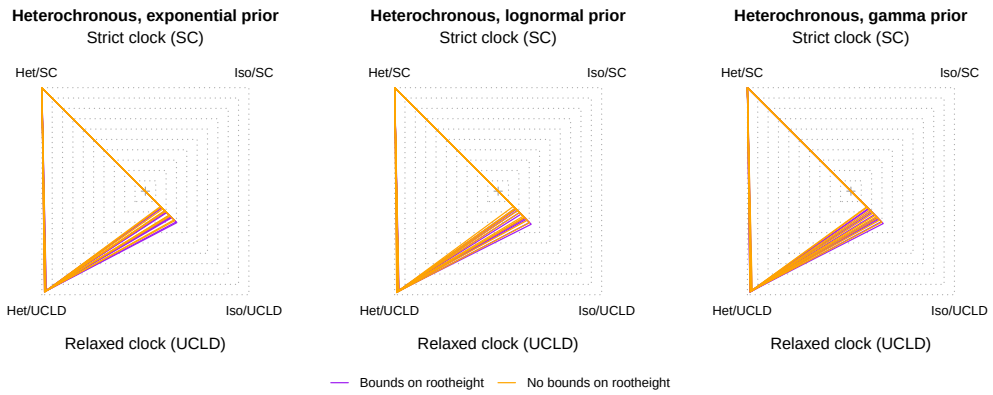


**Fig 2. Relative log marginal likelihoods of simulations with temporal signal.** The polygons represent the relative log marginal likelihood under three possible priors on the effective population size ($\theta$) parameter of the constant-size coalescent tree prior. Each corner corresponds to a combination of model and sampling times, either a strict (SC) or relaxed molecular clock with an underlying log-normal distribution (UCLD), and with (heterochronous) or without (isochronous) sampling times. The correct model used to generate the data is the SC heterochronous. Each polygon is for one simulation replicate (a total of ten) and the colours denote whether we employed a hard bound on the root height of the form Uniform(0.0, 5.0), in blue, or not, in orange.

also worthwhile to note that in general, analyses under the relaxed clock tended to have fewer type I classification errors (for data sets with no temporal signal) than the strict clock, regardless of the true molecular clock model used to generate the data.

**Table 4. Correctly classified simulation replicates under isochronous trees.** A total of ten simulations were generated in each case, under isochronous trees, such that they are not expected to support temporal signal. A number of ten represents perfect classification according to the Bayesian evaluation of temporal signal, BETS and a log Bayes factor of at most -3.2 (strong evidence against temporal signal). The rows correspond to three possible priors on the effective population size of the constant-size coalescent, $\theta$. The 'Best clock model' is a situation where we consider the best heterochronous and isochronous model, take their log Bayes factor, and determine a lack of temporal signal if it is at most -3.2.

| **True clock model; clock model in analysis** | Exponential | Γ | Log-normal |
|---|---|---|---|
| Strict clock; Strict clock | 10 | 0 | 0 |
| Strict clock; Relaxed clock | 10 | 10 | 10 |
| Strict clock; Best clock model | 10 | 0 | 0 |
| Relaxed clock; Strict clock | 10 | 0 | 0 |
| Relaxed clock; Relaxed clock | 10 | 9 | 9 |
| Relaxed clock; Best clock model | 10 | 0 | 1 |

Our simulation results demonstrate that detecting temporal signal when it is not

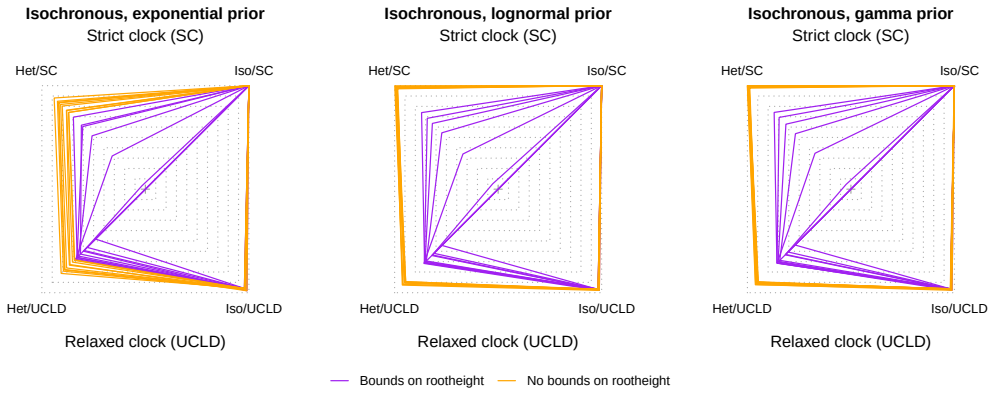


**Fig 3. Relative log marginal likelihoods of simulations with no temporal signal.** The polygons here represent the same information as in Fig 2. The correct model used to generate the data here is the SC isochronous (ultrametric).

present (type I error), is more common under some prior configurations (here the Γ and log-normal priors on $\theta$) than the opposite (type II error, failing to detect temporal signal when it is present). Upon inspecting the resulting phylogenetic trees and the posterior of key parameters we found a probable cause. The incorrect inclusion of sampling times produces a dramatic overestimation of the height of the tree, especially under the strict molecular clock model, a phenomenon that we refer to as 'tree extension' (Fig 4). Under this situation, the sampling times represent such a small proportion of the root height (the time from the most recently sampled node and the root-node), that the heterochronous tree is indistinguishable from one that is ultrametric and thus the log marginal likelihoods of a model with sampling times can be comparable, or higher than that for a model without sampling times. In fact, in Fig 4 the sampling times span 0.5 units of time, such that they represent only 0.05% of the total height of a tree height of 1,000 units of time. The phenomenon of tree extension also occurs under the relaxed molecular clock, but to a much lesser extent, and thus under this model it is easier to correctly classify isochronous data sets, because incorrect sampling times are effectively penalised.

A problem with fixing the clock rate to 1.0 for the isochronous analyses is that the branch lengths of the time-tree will be expressed in units of subs/site. The $\theta$ parameter of the constant-size coalescent is proportional to units of time [26,34] (as are most other parameters of the tree prior, for example the growth rate of the exponential-growth coalescent). When time-calibrations are used $\theta$ corresponds to the population size multiplied by the generation time ($N_e \times$ generation time). Thus, the prior on $\theta$ for the heterochronous and isochronous analyses has different meaning (the branch lengths are in not in the same units). A simple solution is to ensure that this parameter is scaled to match the units of the branch lengths, or to fix the molecular clock rate in the isochronous analyses to a biologically meaningful value. In our simulations we fixed the molecular clock rate to its true value, but we also found that using a number within the expected order of magnitude of the organism in question is sufficient (e.g. $10^{-4}$ to $10^{-3}$ subs/site/year for a ssRNA virus).

Our results indicate that using priors that favour plausible node heights is important

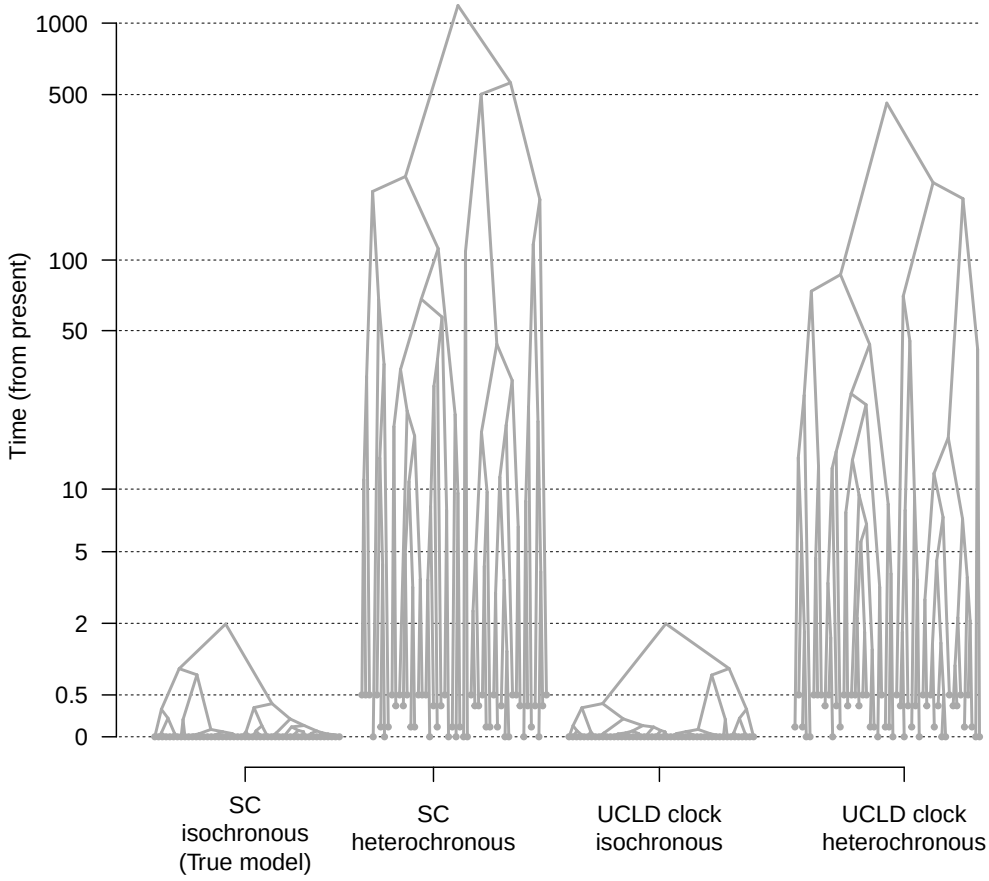


**Fig 4. Phylogenetic tree extension for a simulation replicate with no temporal signal**. Highest clade credibility trees from a data set simulated with no sampling times (isochronous) and under a strict molecular clock model (SC). The prior on $\theta$ is a $\Gamma(\kappa = 0.001, \theta = 1000)$, which resulted in high classification errors using BETS. The y-axis is the time from the present. Tip nodes have solid grey circles. Including sampling times that span 0.5 units of time and about 1/4 of the true root height induces dramatic overestimation of the root height, compared to the true model (SC, isochronous). This effect occurs under both molecular clock models, the SC and the relaxed molecular clock with an underlying log-normal distribution (UCLD), but it is markedly less pronounced in the UCLD. Note that the y-axis is in logarithmic scale ($\log_{10}$).

to ensure the accuracy of temporal signal detection. However, the interplay between the parameters of the tree prior and the resulting tree topologies and node heights is not necessarily trivial, particularly when the tree prior involves multiple parameters. Thus, defining suitable priors for the parameters of the tree prior requires careful attention. A pragmatic solution is to include additional prior information in the form of hard bounds on the root-height or the molecular clock rate. To this end, we investigated the effect of including a uniform prior between 0.0 and 5.0 units of time for the root height, meaning that trees that are older than 5.0 units have a prior probability of 0.0. Crucially, the

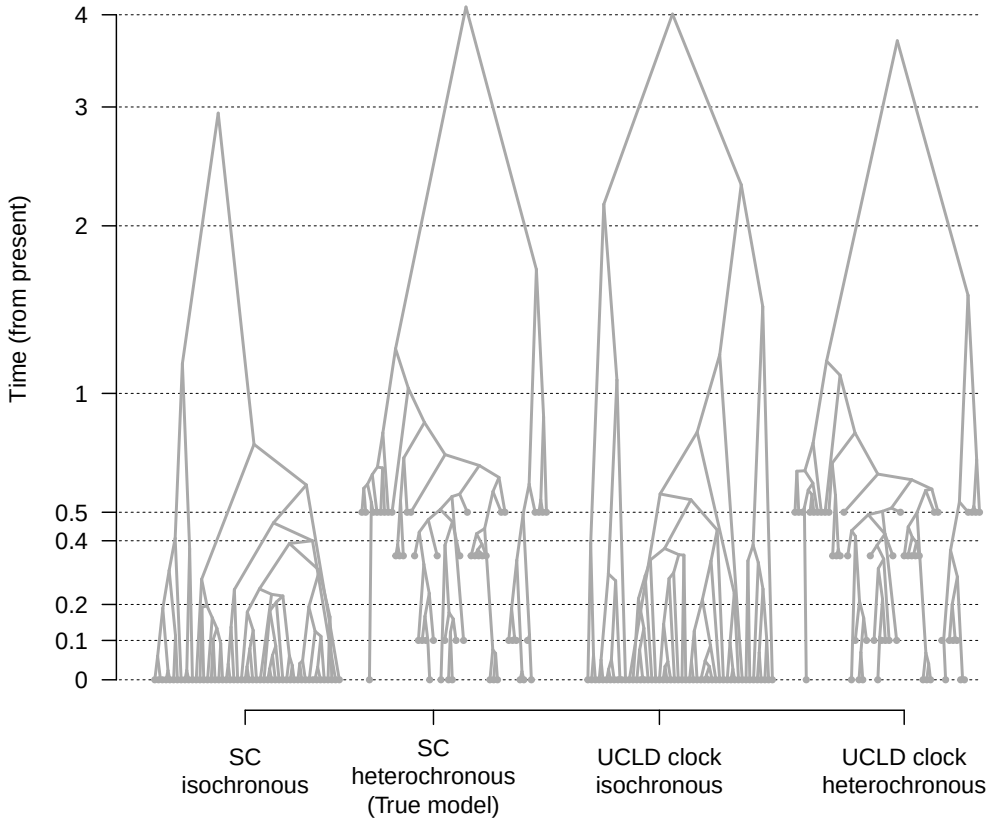


**Fig 5. Phylogenetic trees from a simulation replicate with temporal signal**. Highest clade credibility trees from a data set simulated with sampling times (heterochronous) and under a strict molecular clock model (SC). The isochronous trees are inferred by fixing the molecular clock rate to the true value, such that the timescale is in the comparable units to the heterochronous analyses. Unlike the estimates for isochronous trees (e.g. Fig 4), the height of the trees under all scenarios are comparable. Axes and labels are the same as those of Fig 4

trees under which we generated our simulated data had root heights of around 2.0 units of time, and thus the hard bound of 5.0 allows for trees that are over twice as old as the truth.

Setting hard bounds on the root height resulted in perfect classification accuracy for both, the heterochronous and isochronous simulations (Table 5 and Fig 2, and Table 6 and Fig 3, respectively). The improvement in classification for data sets with no temporal signal is likely because the hard bounds prevent the tree extension phenomenon, and thereby including sampling times imposes a penalty on the log marginal likelihood (see polygons in Fig 2). Our empirical data set of *V. cholerae*, which had evidence of temporal signal under all prior conditions, also displayed strong evidence for temporal signal with a hard bound on of 500 years before present on the root height (all log Bayes factors were at least 200 in favour of temporal signal).

**Table 5. Correctly classified simulation replicates under heterochronous trees using hard bounds on the root height.** Rows and columns are identical to those of Table 3, but here the heterochronous analyses include an explicit prior on the root height, via a uniform distribution between 0 and 5.0.

| **True clock model; clock model in analysis** | Exponential | Γ | Log-normal |
|---|---|---|---|
| Strict clock; Strict clock | 10 | 10 | 10 |
| Strict clock; Relaxed clock | 10 | 10 | 10 |
| Strict clock; Best clock model | 10 | 10 | 10 |
| Relaxed clock; Strict clock | 10 | 10 | 10 |
| Relaxed clock; Relaxed clock | 10 | 10 | 10 |
| Relaxed clock; Best clock model | 10 | 10 | 10 |

**Table 6. Correctly classified simulation replicates under isochronous trees using hard bounds on the root height.** Rows and columns are identical to those of Table 4, but here the heterochronous analyses include an explicit prior on the root height, via a uniform distribution between 0 and 5.0.

| **True clock model; clock model in analysis** | Exponential | Γ | Log-normal |
|---|---|---|---|
| Strict clock; Strict clock | 10 | 10 | 10 |
| Strict clock; Relaxed clock | 10 | 10 | 10 |
| Strict clock; Best clock model | 10 | 10 | 10 |
| Relaxed clock; Strict clock | 10 | 10 | 10 |
| Relaxed clock; Relaxed clock | 10 | 10 | 10 |
| Relaxed clock; Best clock model | 10 | 10 | 10 |

The exponential-size coalescent is more flexible than the constant-size coalescent, where population size change is allowed to change deterministically (for its description in a phylodynamic context see [35, 36]). This model has two key parameters, the 'scaled population size' ($\Phi$) and the exponential 'growth rate' ($r$). Due to its coalescent nature the time to the most recent common ancestor scales positively with $\Phi$. We investigated the performance of BETS under this tree prior, using the same three prior distributions on $\Phi$ as we did for $\theta$ in the constant-size coalescent and for the growth rate we used $Laplace(\mu = 0.0, b = 1.0)$. The relative log marginal likelihoods between models were very similar to those using the constant-size coalescent. Heterochronous data sets were overwhelmingly classified as having temporal signal, whereas in isochronous data sets using hard bounds correctly improved support for a lack of temporal signal (Supporting information).

## Prior predictive simulations and parameter correlations

Our finding that the tree prior can affect model selection prompted an investigation of parameter interactions and of the expectations under the prior. We simulated phylogenetic trees from a prior distribution to inspect the correlation of parameters and the marginal prior for those that have obvious associations (e.g. the evolutionary rate has a CTMC-rate reference prior that depends on tree length). These simulations are commonly known as prior predictive simulations (e.g. [37]), and referred to as 'sampling from the prior' in the phylogenetics literature [38]. Initially, we set a uniform prior on $\theta$ from 0 to $10^3$ and recorded the evolutionary rate, the tree length and root height. This prior is not generally recommended [39], and we present it here to illustrate correlations

between parameters and the marginal prior, instead of using it for analysing our data.

An obvious finding is a natural positive correlation between tree length, root height, although the trends is not strictly linear (Fig 6). We also observed a positive correlation between $\theta$, tree length and tree height, which is also expected because large population sizes impose long coalescent times [40]. The nature of this correlation is heteroskedastic, with the variance in these tree statistics increasing with $\theta$. Our simulations demonstrate an inverse relationship between the evolutionary rate, $\theta$ and the tree statistics, but with a range that can span several orders of magnitude and with values ranging from $10^{-9}$ to $10^{-4}$ subs/site/time, meaning that the CTMC-rate reference prior tends to be diffuse. It is also noteworthy that the uniform prior on $\theta$ does not result in uniform marginal prior distributions for any of the parameters investigated here. These results illustrate the importance of visualising the prior and the fact that it is difficult to predict how different parameters will interact.

We conducted prior predictive simulations for the six prior configurations for $\theta$ under a heterochronous data set. In Fig 7 we show the resulting distribution on the root height. The exponential ($\theta \sim Exponential(\mu = 1.0)$, $\Gamma$ ($\Gamma(\kappa = 0.001, \theta = 1000)$) and log-normal (log-normal($\mu = 1.0, \sigma = 5.0$)) prior distributions respectively produced mean root heights of 2.90 (95% quantile range, qr: 1.62 to 14.34), 1.61 (95% qr: 1.50 to 4.87) and 772.11 (95% qr: 1.66 to $5.06 \times 10^5$) units of time. Clearly, the log-normal is the most vague prior here, but it produces implausible values of several orders of magnitude higher than our expectation of tree heights of around one and ten units of time (as simulated using $\theta = 1.0$).

For comparison, we also simulated trees under the same priors on $\theta$, with hard bounds on the root height, and with a uniform distribution with minimum and maximum values of 0.0 and 5.0, as described above. In this case, the exponential prior on $\theta$ yielded trees with root heights of mean 2.47 (95% qr: 1.62 to 5.16), whereas those for the log-normal and $\Gamma$ were 1.61 (95% qr: 1.50 to 5.11), and 1.96 (95% qr: 1.54 to 4.42), respectively. As a result, in the log-normal prior on $\theta$ the use of hard bounds on the root height resulted in much shorter root heights, with a smaller impact on the exponential and $\Gamma$ priors.

# Discussion

Our study demonstrates that the choice of prior distribution is a key factor for Bayesian model selection and that it can mislead tests of temporal signal. In general, data sets with no temporal signal are easily misclassified when the prior favours an implausibly old root height and low evolutionary rates, resulting in type I errors. The incorrect detection of temporal signal may lead to a systematic overestimation of the evolutionary timescale and an underestimation of the molecular clock rates.

We find that tree extension is the most probable reason for type I errors in BETS, because it reduces the sampling window relative to the root height, such that the trees with sampling times are very similar to ultrametric trees. The phylogenetic likelihood of such overly old trees can be consistent with that from much shorter trees with no sampling times if their evolutionary rate is very low, such that the genetic distance along their branches is comparable.

Our observation of tree extension pertains to isochronous data sets analysed with sampling times, but a similar situation occurs in date-randomisation tests [15]. Here, the sequence sampling times are permuted a number of times, the evolutionary rate is re-estimated, and the data are considered to have temporal signal if the estimates from the permutations do not overlap with that from the correct sampling times. Notably, when the data do have temporal signal, the estimates from the permutations are substantially lower, implying older times to the most recent common ancestor [14].

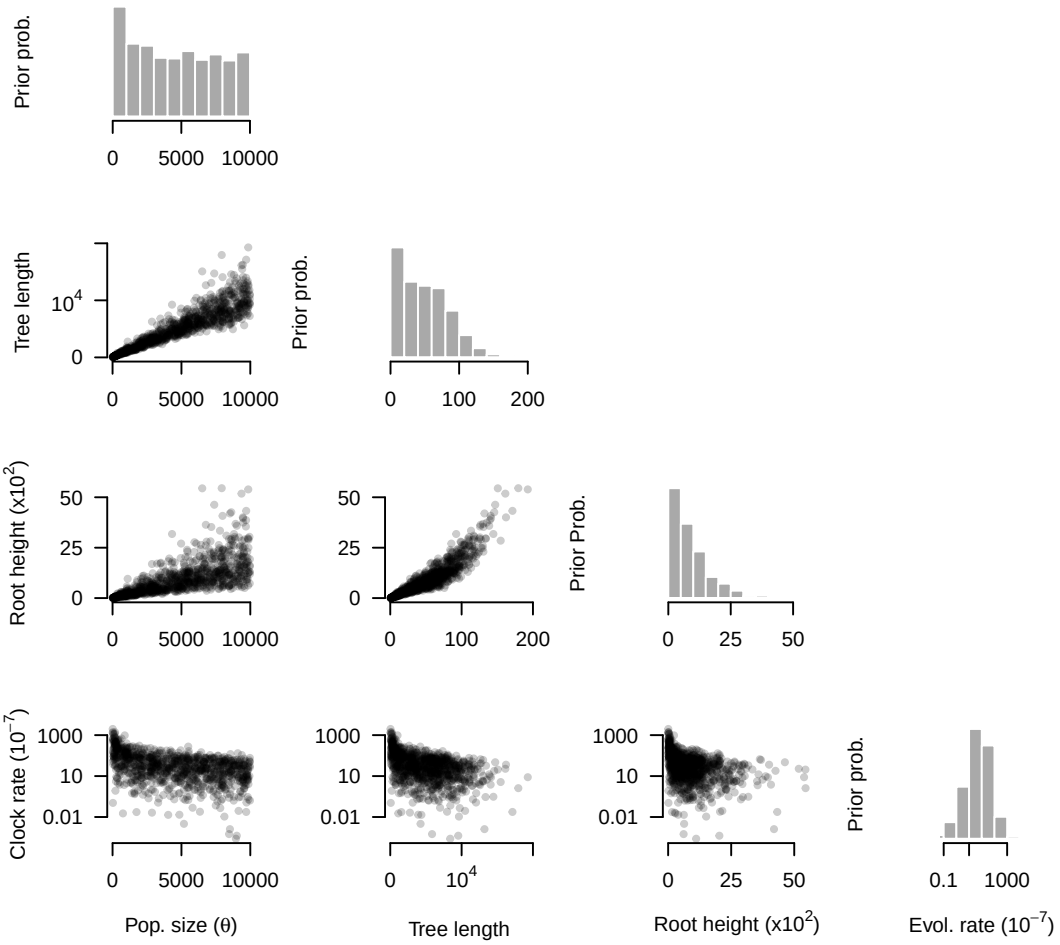


**Fig 6. Marginal prior distributions and pairs plots.** The grey histograms for correspond to the parameter labelled at the bottom of each column; effective population size (pop. size, $\theta$), tree length, root height, and the evolutionary rate (evol. rate). The prior for $\theta$ here is a Uniform distribution between 0 and $10^3$, while that for the evolutionary rate is a CTMC-rate reference prior. Note that the tree length and root height have units of time, the evolutionary rate is in subs/site/time, and $\theta$ is proportional to units of time.

Therefore the incorrect inclusion of incorrect sampling times, whether the data set is truly isochronous or not, may be result in tree extension as a means of compensating for the likelihood penalty imposed by incorrect sampling times.

While the phenomenon of tree extension occurs for the strict and relaxed molecular clock models, it is less pronounced in relaxed molecular clock models (e.g. see Fig 4). We hypothesise that the relaxed molecular clock is more robust to tree extension in data sets that are truly isochronous because this model can absorb the incorrect inclusion of sampling times by treating them as rate variation among lineages.

The presence, rather than the absence, of temporal signal is much easier to detect, meaning low type II errors in BETS. In this case, specifying an incorrect isochronous model does not result in an obvious distortion of the time tree that could mislead BETS, at least under the conditions that we used here. It is conceivable, however, that

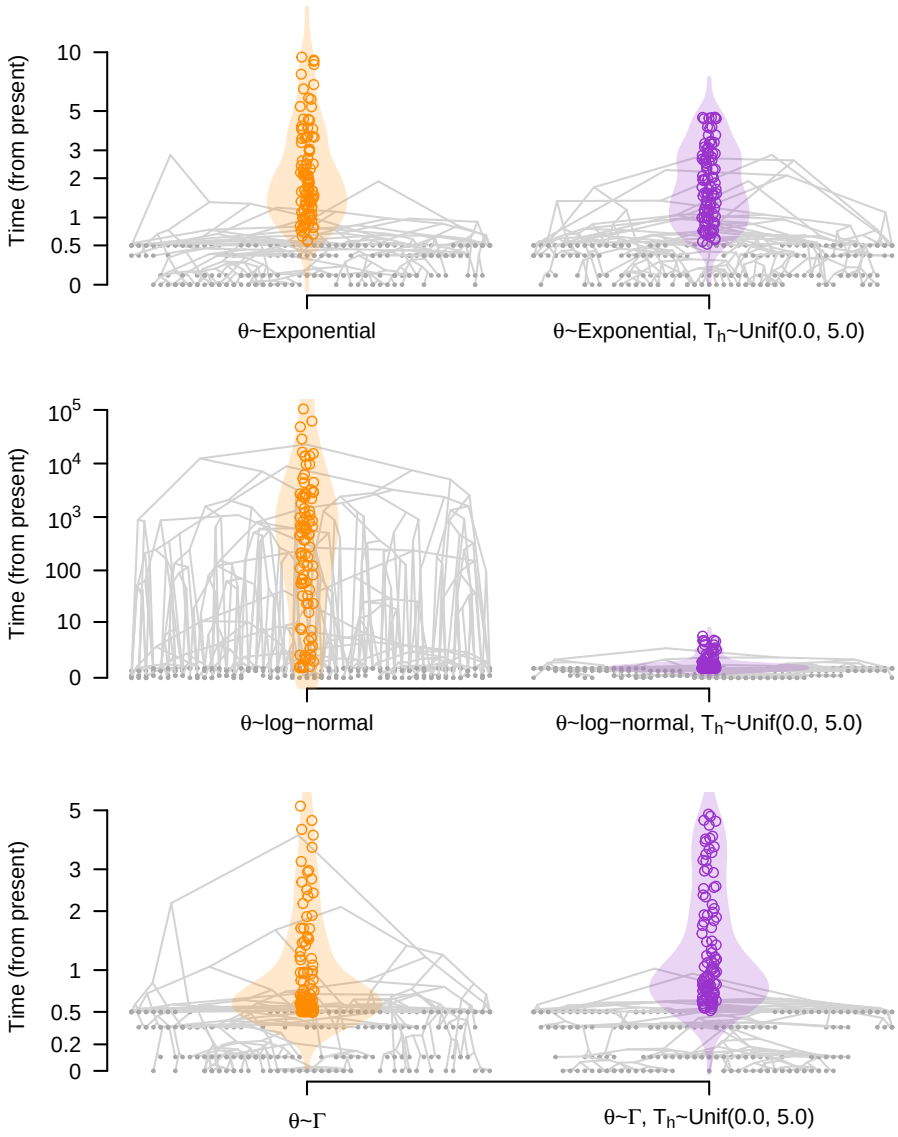


**Fig 7. Prior predictive simulations and marginal priors of root heights, given the prior on the effective population size, $\theta$.** Each panel corresponds to a different prior on $\theta$, as described on Table 1 (Exponential($\mu = 1.0$), Log-normal($\mu$ =1.0, $\sigma$ =5.0), and $\Gamma(\kappa = 0.001, \theta = 1000)$). We show five simulated trees from our analysis using sampling times (heterochronous analyses) and overlaid them (similar to densitree plots [41]). The violin plots show the prior densities of the root height and the hollow circles denote 100 randomly drawn samples from the prior. The y-axis is the time from the present, but note that the scales are different. Tip nodes are shown with solid grey circles. The densities and trees on the left, in orange, do not include an explicit prior on the root height ($T_h$), while those to the right, in purple, have a hard bound on tree height in the form of a uniform prior between 0.0 and 5.0 units of time.

certain priors on the phylogenetic tree or evolutionary rate could result in type II errors.

A key consideration is that the parameters of the tree prior for isochronous and

heterochronous analyses should be in the same units (and of similar magnitude), which facilitates comparison of the models in question. For example, fixing the evolutionary rate to 1.0 in an isochronous analysis means that branch lengths of the time tree are in units of expected genetic distance (usually subs/site) and thus the coalescent parameters have a different meaning to those estimated under heterochronous analyses (where the evolutionary rate is a free parameter). A more tractable approach is to conduct isochronous analyses by fixing the evolutionary rate to a value within the expected order of magnitude. Biological knowledge, such as the negative correlation between genome size and rates of microbes [33, 42] or simply a previous estimate for a closely related organism, can be helpful for specifying such values.

Our results point to a few recommendations to improve tests of temporal signal. First, careful researchers should carefully elicit the priors, which appears important for Bayesian model selection (see [43] for a related problem in tree topology tests). Prior predictive simulations are essential to understand potential interactions between model parameters and ultimately whether the prior expectation is reasonable with respect to our knowledge about the data. For instance, in our simulation study, using hard bounds on the tree height alleviated the problem of tree extension when the prior on $\theta$ favoured very old trees. In empirical data, however, one may not want to make such strong statements, and prior predictive simulations can help determine whether the tree prior and associated parameters produce trees with sensible root heights (e.g. the exponential prior on $\theta$ had low type I and type II errors in our simulations).

Our second recommendation is to conduct prior sensitivity analyses on a set of candiate priors to determine the extent to which the prior can influence the posterior [44, 45], and model selection using Bayes factors [46]. Visualising the posterior and prior distributions for a range of priors can be illuminating (see Supporting information). A prior that makes unreasonable statements and is overly influential on the posterior may need to be revised. The exponential prior on $\theta$ in the *Powassan virus* did not support temporal signal, but note that it is much more influential on the posterior than the $\Gamma$ and log-normal priors for this particular data set. In contrast, the *V. cholerae* data seemed robust to the three priors that we used. Some empirical data sets yielded unclear evidence for temporal signal according to BETS, such as the *T. pallidium* data set that we reanalysed. In such cases, the decision of whether the data have sufficient temporal signal may require multiple lines of evidence, such as date-randomisation tests [15, 16], comparisons of the prior and posterior [47], and root-to-tip regressions. [10, 11]. When temporal signal in inconclusive, the inclusion of additional information, such as internal node calibrations, and informative molecular clock rate priors may be essential for molecular dating, as was the case in that study [22].

Finally, we find that the choice of the molecular clock model has a tangible impact on tests of temporal signal. The strict molecular clock model is more prone to type I error than the relaxed molecular clock model. The most likely reason for this finding is that this approach mitigates tree extension when the data have no temporal signal. Thus we recommend that, where possible, the results of BETS be considered under a relaxed molecular clock model.

The sum of our results and recommendations has implications for the reliability of estimates of evolutionary rates and timescales, for determining whether a population is measurably evolving, and even for assessing the phylodynamic threshold of emerging microbes [48]. Concretely, genome data from recently emerging microbes may have very few substitutions, in which case prior sensitivity analyses and prior predictive simulations would easily reveal whether the data are sufficiently informative. Overall, tests of temporal signal have a key place in genomic analyses of pathogens and our results will be useful as guidelines to improve their application and interpretation.

# Materials and methods

## Empirical data

We selected three different datasets to evaluate temporal signal, *V. cholerae* [21], *Powassan virus* [23], and *T. pallidum* [22]. These varied in their sampling timeframe, number of informative sites, and number of sequences. The most sparse dataset was *T. pallidum*, where sampling dates spanned 481 years (1534 to 2016), with 28 sequences each containing 1,500 SNP sites. Among these samples, there were only two in the 1500's and two in the 1700's, with the rest of the samples concentrated in the 1900's to 2000's. There were 319 sequences with 11,193 sites (the complete genome) for *Powassan virus*, spanning 24 years of sampling times (1995 to 2019). Most of the samples were collected after 2010, with only three isolated in 1995. For *V. cholera* we had 122 sequences with 1,57 SNP sites across 73 years of sampling (1937 to 2010). There are 1,392 unique site patterns in *V. cholera*, 3,457 in *Powassan virus*, and 840 in *T. pallidum*.

For *V. cholerae* and *T. pallidum* our data consisted of SNP sites. To account for such ascertainment bias, we specified the number of constant nucleotides in the whole genome in our subsequent analyses. We sampled the posterior distribution using Markov chain Monte Carlo as implemented in BEAST1.10. The chain length was $10^8$ steps, sampling every $10^3$ to draw a total of $10^4$ samples. The prior for the evolutionary rate of the strict clock was a CTMC-rate reference prior (i.e. a $\Gamma(\alpha = 0.5, \beta =$tree length, and mean$=\alpha/\beta$) [30]. For the log-normal distribution of the relaxed clock we also used the CTMC-rate reference prior for the mean rate (known as the ucld.mean in the program) and an exponential prior with mean 0.33 for the standard deviation (the ucld.stdev in the program). For the tree prior we used a constant-size coalescent with population size, $\theta$ with three possible priors, as described in Table 1. In all cases we used the HKY+$\Gamma_4$ substitution model, with the default priors in BEAST1.10.

To calculate log marginal likelihoods we used generalised stepping-stone [49, 50]. This method requires a working distribution for all parameters, including the tree prior, for which we used the matching coalescent model. We set 100 path steps between the unnormalised posterior and the working distribution, following equally spaced intervals from a $\beta(0.3, 1.0)$ distribution. For each step we ran a chain length of $2\times10^6$ steps. We considered these settings to be appropriate after repeating the log marginal likelihood calculations 10 times for two of data sets and ensuring that the values did not vary by more than 1.0 log likelihood units.

## Simulation experiments

For our simulations we considered well-understood conditions to isolate the impact of the tree prior on tests of temporal signal. We simulated phylogenetic trees under a constant-size coalescent model with a fixed population size of 1.0 and a resulting average root height of 2.0 units of time. The trees could be isochronous (i.e. ultrametric) or heterochronous. For the latter we assigned tip heights of of 0.0, 0.10, 0.35, or 0.50, with equal probability. This situation implies four discrete sampling periods, which resembles sequencing blitzes [51], or archaeological sampling of strata [52]. Because the coalescent model used to analyse the data is conditioned on sampling times we expect it to be robust to such sampling bias [53–55]. We used a JC substitution model [56] to generate sequence alignments of 1,000 nucleotides and an evolutionary rate of 0.05 subs/site/time, which resulted in around 250 unique site patterns. For our simulations under a relaxed molecular clock model we sampled branch rates from a log-normal distribution with mean 0.05 and standard deviation of 0.25. The procedure for obtaining the simulated alignments consisted of specifying the model

above in BEAST1.10 with an empty sequence alignment to sample phylogenetic trees. We then used NELSI [57] and Phangorn [58] to simulate evolutionary rates (a single value for the strict clock and the branch rates for the relaxed molecular clock model) and sequence alignments, respectively.

We analysed the simulated data under heterochronous and isochronous models. For the heterochronous analyses we used the correct sampling times (where the correct model was the heterochronous) or assigned the tip heights above randomly (0.0, 0.10, 0.35, or 0.50) where the isochronous was the true model. For the evolutionary rate (clock.rate in the strict and ucld.mean for the relaxed molecular clock model) we set the default CTMC-rate reference prior and the six possible configurations of the prior on $\theta$ (Table 1, plus those with hard bounds on the root height). For the isochronous analyses we did not specify sampling times and we fixed evolutionary rate to its true value of 0.05 to ensure that the branch lengths, $\theta$ and other parameters are in the correct units. We calculated log marginal likelihoods with the same procedure as for the empirical data.

# Supporting information

**S1 Fig.**

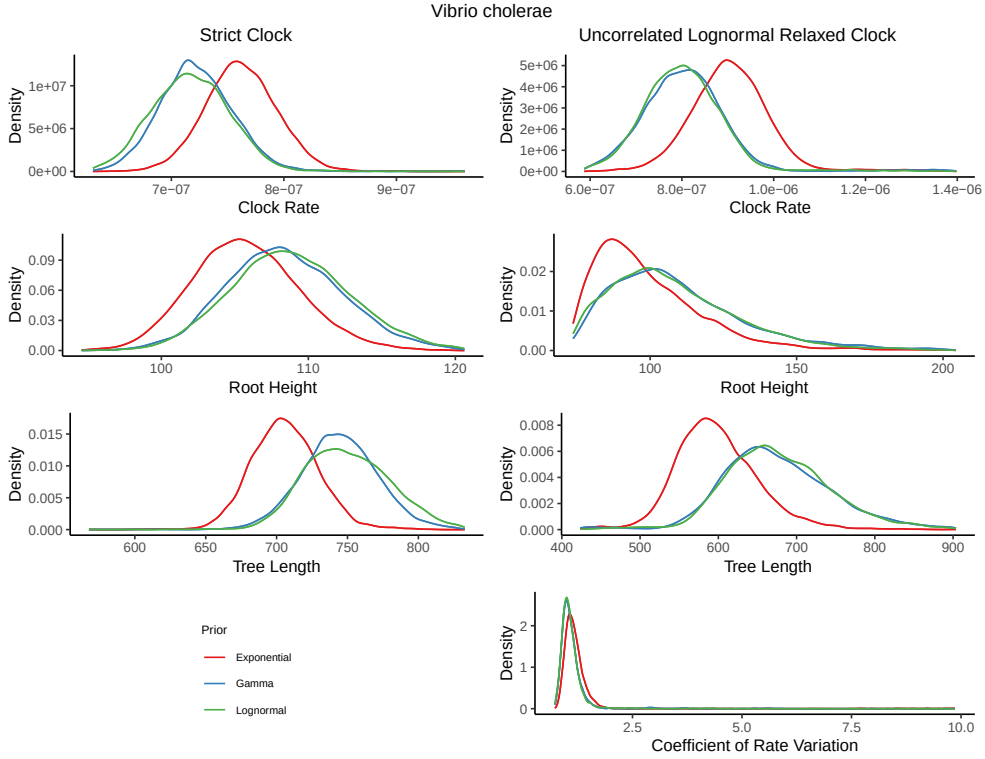


**Densities of key statistics of cholera empirical data.** The clock rate, root height, tree length, and coefficient of rate variation are shown under three priors on $\theta$, exponential (red), gamma (blue), and lognormal (green).

**S2 Fig.**

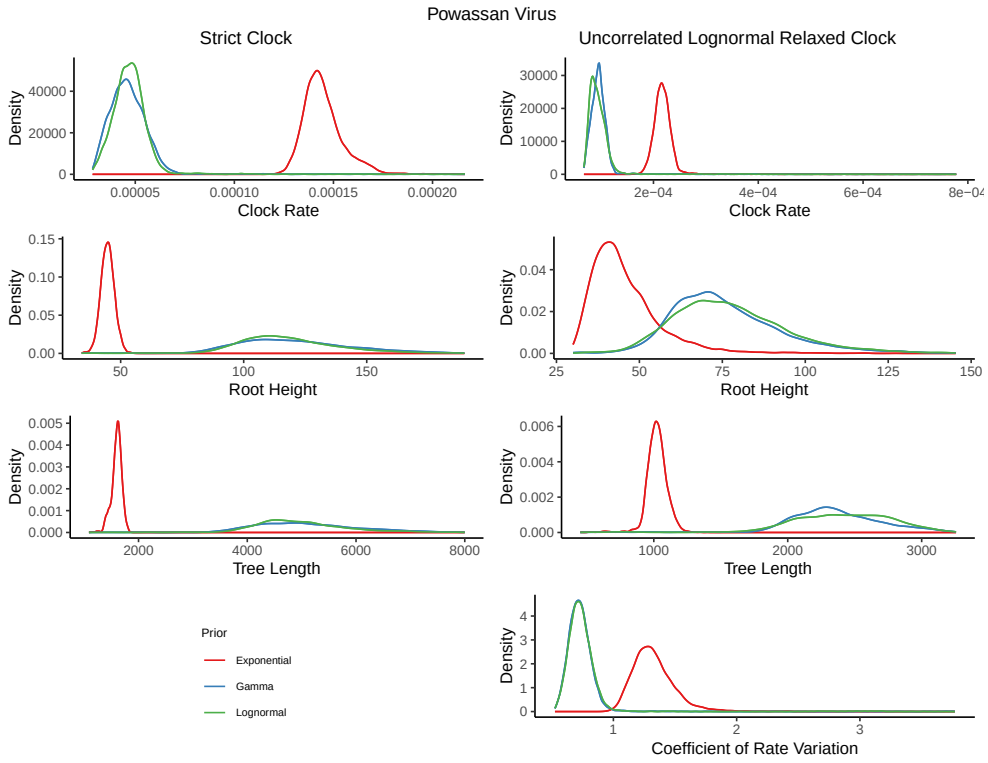


**Densities of key statistics of *Powassan virus* empirical data.** The clock rate, root height, tree length, and coefficient of rate variation are shown under three priors on $\theta$, exponential (red), gamma (blue), and lognormal (green).

**S3 Fig.**

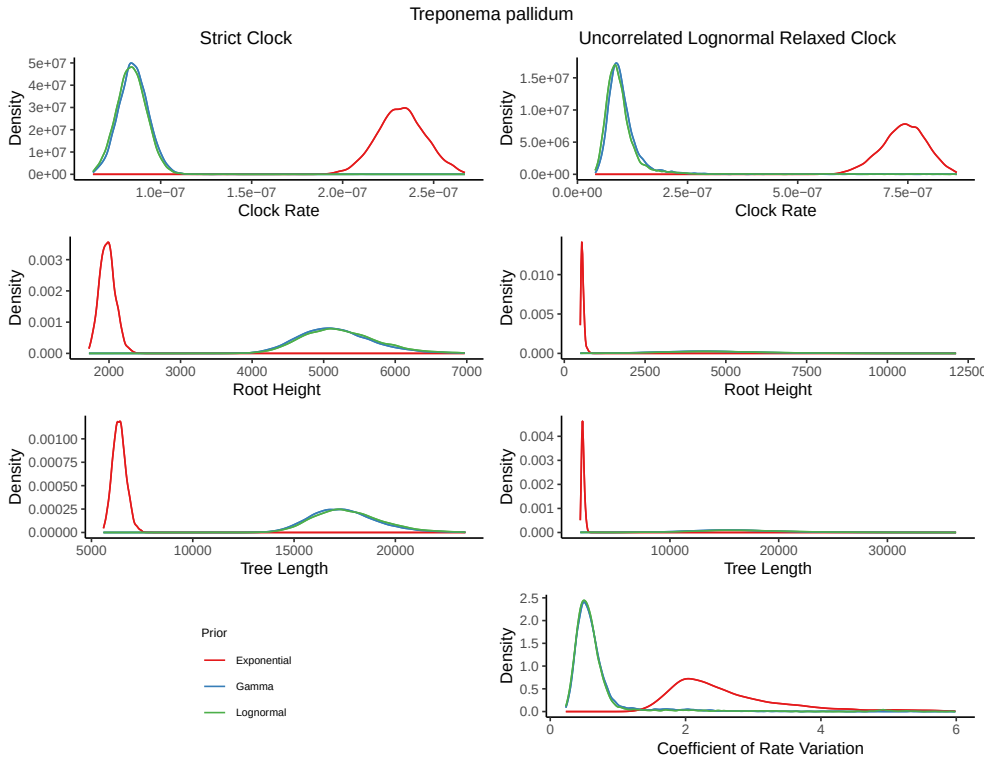


**Densities of key statistics of *Treponema palladium* empirical data.** The clock rate, root height, tree length, and coefficient of rate variation are shown under three priors on $\theta$, exponential (red), gamma (blue), and lognormal (green).

**S4 Fig.**

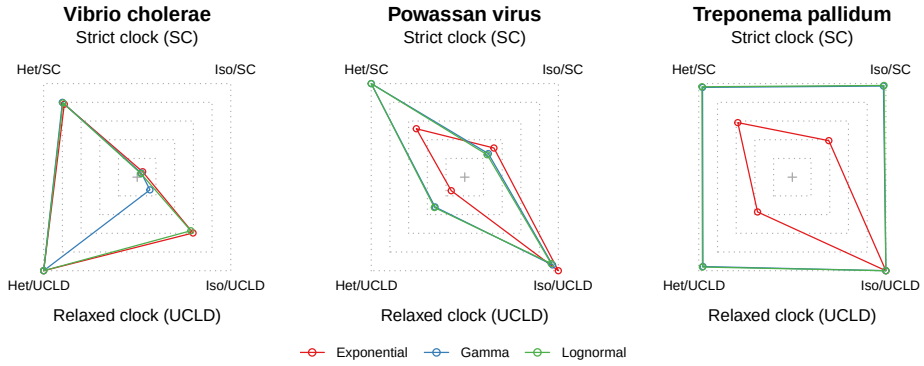


**Relative log marginal likelihoods of empirical data sets with bounds on root height.** The polygons represent the relative log marginal likelihoods of each microbe dataset under a different effective population size ($\theta$) prior, analysed with four different configurations. Het (heterochronous) includes sampling, while iso (isochronous) does not include any sampling times. SC is strict clock and UCLD is the uncorrelated lognormal relaxed clock. Red represents an exponential prior on the effective population size, blue is a $\Gamma$ prior, and green is a log-normal prior.

**S5 Fig.**

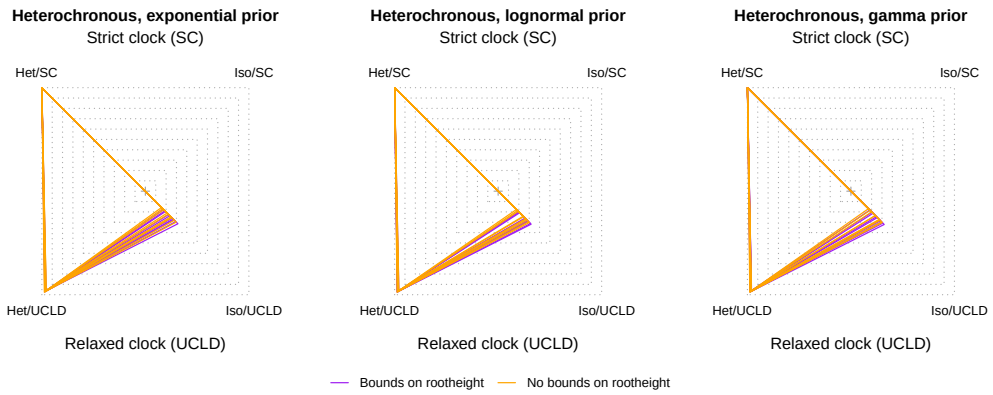


**Fig 8. Relative log marginal likelihoods of simulations with temporal signal and analysed under an exponential-size coalescent tree prior.** The polygons represent the relative log marginal likelihood under three possible priors on the effective population size ($\theta$) parameter of the constant-size coalescent tree prior. Each corner corresponds to a combination of model and sampling times, either a strict (SC) or relaxed molecular clock with an underlying log-normal distribution (UCLD), and with (heterochronous) or without (isochronous) sampling times. The correct model used to generate the data is the SC heterochronous. Each polygon is for one simulation replicate (a total of ten) and the colours denote whether we employed a hard bound on the root height of the form Uniform(0.0, 5.0), in blue, or not, in orange.

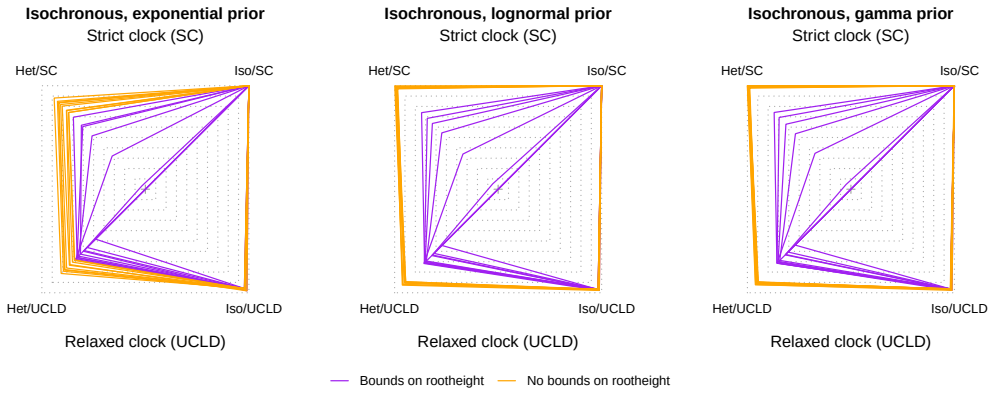


**Fig 9. Relative log marginal likelihoods of simulations with no temporal signal and analysed under an exponential-size coalescent tree prior.** The polygons here represent the same information as in Fig 8. The correct model used to generate the data here is the SC isochronous (ultrametric).

**S6 Fig.**

## Acknowledgments

This work was supported by the Inception program [Investissement d'Avenir grant ANR-16-CONV-0005], the Australian National Health and Medical Research Council [2017284], and the Australian Research Council [FT220100629].

## References

1. Zuckerkandl E, Pauling L. Evolutionary divergence and convergence in proteins. In: Evolving genes and proteins. Elsevier; 1965. p. 97–166.
2. Drummond AJ, Ho SYW, Phillips MJ, Rambaut A. Relaxed phylogenetics and dating with confidence. PLoS Biology. 2006;4(5):e88.
3. Ho SY, Duchêne S. Molecular-clock methods for estimating evolutionary rates and timescales. Molecular Ecology. 2014;23(24):5947–5965.
4. Yang Z, Rannala B. Bayesian estimation of species divergence times under a molecular clock using multiple fossil calibrations with soft bounds. Molecular biology and evolution. 2006;23(1):212–226.
5. Dos Reis M, Yang Z. The unbearable uncertainty of Bayesian divergence time estimation. Journal of Systematics and Evolution. 2013;51(1):30–43.
6. Rodrigo AG, Felsenstein J. Coalescent approaches to HIV population genetics. The evolution of HIV. 1999; p. 233–272.
7. Korber B, Muldoon M, Theiler J, Gao F, Gupta R, Lapedes A, et al. Timing the ancestor of the HIV-1 pandemic strains. science. 2000;288(5472):1789–1796.
8. Drummond AJ, Pybus OG, Rambaut A, Forsberg R, Rodrigo AG. Measurably evolving populations. Trends in ecology & evolution. 2003;18(9):481–488.
9. Biek R, Pybus OG, Lloyd-Smith JO, Didelot X. Measurably evolving pathogens in the genomic era. Trends in ecology & evolution. 2015;30(6):306–313.
10. Rambaut A, Lam TT, Max Carvalho L, Pybus OG. Exploring the temporal structure of heterochronous sequences using TempEst (formerly Path-O-Gen). Virus evolution. 2016;2(1):vew007.
11. Featherstone LA, Rambaut A, Duchene S, Wirth W. Clockor2: Inferring global and local strict molecular clocks using root-to-tip regression. BioRxiv. 2023; p. 2023–07.
12. Volz E, Frost SD. Scalable relaxed clock phylogenetic dating. Virus evolution. 2017;3(2):vex025.
13. Doizy A, Prin A, Cornu G, Chiroleu F, Rieux A. Phylostems: a new graphical tool to investigate temporal signal of heterochronous sequences datasets. Bioinformatics Advances. 2023;3(1):vbad026.
14. Rieux A, Balloux F. Inferences from tip-calibrated phylogenies: a review and a practical guide. Molecular ecology. 2016;25(9):1911–1924.
15. Ramsden C, Holmes EC, Charleston MA. Hantavirus evolution in relation to its rodent and insectivore hosts: no evidence for codivergence. Molecular biology and evolution. 2009;26(1):143–153.

16. Duchêne S, Duchêne D, Holmes EC, Ho SY. The performance of the date-randomization test in phylogenetic analyses of time-structured virus data. Molecular Biology and Evolution. 2015;32(7):1895–1906.

17. Duchene S, Lemey P, Stadler T, Ho SY, Duchene DA, Dhanasekaran V, et al. Bayesian evaluation of temporal signal in measurably evolving populations. Molecular Biology and Evolution. 2020;37(11):3363–3379.

18. Molak M, Suchard MA, Ho SY, Beilman DW, Shapiro B. Empirical calibrated radiocarbon sampler: a tool for incorporating radiocarbon-date and calibration error into B ayesian phylogenetic analyses of ancient DNA. Molecular ecology resources. 2015;15(1):81–86.

19. Gelman A, Rubin DB. Avoiding model selection in Bayesian social research. Sociological methodology. 1995;25:165–173.

20. Gelman A, Carlin JB, Stern HS, Rubin DB. Bayesian data analysis; 2014.

21. Devault AM, Golding GB, Waglechner N, Enk JM, Kuch M, Tien JH, et al. Second-pandemic strain of Vibrio cholerae from the Philadelphia cholera outbreak of 1849. New England Journal of Medicine. 2014;370(4):334–340.

22. Majander K, Pfrengle S, Kocher A, Neukamm J, Du Plessis L, Pla-Díaz M, et al. Ancient bacterial genomes reveal a high diversity of Treponema pallidum strains in early modern Europe. Current Biology. 2020;30(19):3788–3803.

23. Vogels CB, Brackney DE, Dupuis AP, Robich RM, Fauver JR, Brito AF, et al. Phylogeographic reconstruction of the emergence and spread of Powassan virus in the northeastern United States. Proceedings of the National Academy of Sciences. 2023;120(16):e2218012120.

24. Suchard MA, Lemey P, Baele G, Ayres DL, Drummond AJ, Rambaut A. Bayesian phylogenetic and phylodynamic data integration using BEAST 1.10. Virus Evolution. 2018;4(1):vey016.

25. Boskova V, Bonhoeffer S, Stadler T. Inference of epidemiological dynamics based on simulated phylogenies using birth-death and coalescent models. PLoS Computational Biology. 2014;10(11):e1003913.

26. Drummond AJ, Nicholls GK, Rodrigo AG, Solomon W. Estimating mutation parameters, population history and genealogy simultaneously from temporally spaced sequence data. Genetics. 2002;161(3):1307–1320.

27. R Oaks J, A Cobb K, N Minin V, D Leaché A. Marginal likelihoods in phylogenetics: a review of methods and applications. Systematic Biology. 2019;68(5):681–697.

28. Baele G, Li WLS, Drummond AJ, Suchard MA, Lemey P. Accurate model selection of relaxed molecular clocks in Bayesian phylogenetics. Molecular Biology and Evolution. 2013;30(2):239–243. doi:10.1093/molbev/mss243.

29. Wang Y, Yang Z. Priors in Bayesian phylogenetics. Bayesian phylogenetics: methods, algorithms, and applications. 2014; p. 5–24.

30. Ferreira MA, Suchard MA. Bayesian analysis of elapsed times in continuous-time Markov chains. Canadian Journal of Statistics. 2008;36(3):355–368.

31. Tay JH, Baele G, Duchene S. Detecting episodic evolution through Bayesian inference of molecular clock models. Molecular Biology and Evolution. 2023;40(10):msad212.

32. Kass RE, Raftery AE. Bayes factors. Journal of the American Statistical Association. 1995;90(430):773–795.

33. Duchêne S, Holt KE, Weill FX, Le Hello S, Hawkey J, Edwards DJ, et al. Genome-scale rates of evolutionary change in bacteria. Microbial genomics. 2016;2(11):e000094.

34. Ho SY, Shapiro B. Skyline-plot methods for estimating demographic history from nucleotide sequences. Molecular ecology resources. 2011;11(3):423–434.

35. Volz EM. Complex population dynamics and the coalescent under neutrality. Genetics. 2012;190(1):187–201.

36. Dearlove B, Wilson DJ. Coalescent inference for infectious disease: meta-analysis of hepatitis C. Philosophical Transactions of the Royal Society B: Biological Sciences. 2013;368(1614):20120314.

37. Wesner JS, Pomeranz JP. Choosing priors in Bayesian ecological models by simulating from the prior predictive distribution. Ecosphere. 2021;12(9):e03739.

38. Nascimento FF, Reis Md, Yang Z. A biologist's guide to Bayesian phylogenetic analysis. Nature ecology & evolution. 2017;1(10):1446–1454.

39. Bouckaert RR. Tree priors and dating; 2021. Available from: `beast2.blogs.auckland.ac.nz/tree-priors-and-dating/`.

40. Rosenberg NA, Nordborg M. Genealogical trees, coalescent theory and the analysis of genetic polymorphisms. Nature Reviews Genetics. 2002;3(5):380–390.

41. Bouckaert RR. DensiTree: making sense of sets of phylogenetic trees. Bioinformatics. 2010;26(10):1372–1373.

42. Sanjuán R. From molecular genetics to phylodynamics: evolutionary relevance of mutation rates across viruses. PLoS pathogens. 2012;8(5):e1002685.

43. Bergsten J, Nilsson AN, Ronquist F. Bayesian tests of topology hypotheses with an example from diving beetles. Systematic biology. 2013;62(5):660–673.

44. Foster CS, Sauquet H, Van der Merwe M, McPherson H, Rossetto M, Ho SY. Evaluating the impact of genomic data and priors on Bayesian estimates of the angiosperm evolutionary timescale. Systematic Biology. 2017;66(3):338–351.

45. Lopes HF, Tobias JL. Confronting prior convictions: On issues of prior sensitivity and likelihood robustness in Bayesian analysis. Annu Rev Econ. 2011;3(1):107–131.

46. Lambert B. A student's guide to Bayesian statistics. London: SAGE Publications Ltd; 2018.

47. Duchene S, Duchene DA. Estimating evolutionary rates and timescales from time-stamped data. The Molecular Evolutionary Clock: Theory and Practice. 2020; p. 157–174.

48. Duchene S, Featherstone L, Haritopoulou-Sinanidou M, Rambaut A, Lemey P, Baele G. Temporal signal and the phylodynamic threshold of SARS-CoV-2. Virus Evolution. 2020;6(2):veaa061.

49. Baele G, Lemey P, Suchard MA. Genealogical working distributions for Bayesian model testing with phylogenetic uncertainty. Systematic Biology. 2016;65(2):250–264.

50. Fan Y, Wu R, Chen MH, Kuo L, Lewis PO. Choosing among partition models in Bayesian phylogenetics. Molecular Biology and Evolution. 2011;28(1):523–532.

51. Porter AF, Sherry N, Andersson P, Johnson SA, Duchene S, Howden BP. New rules for genomics-informed COVID-19 responses–lessons learned from the first waves of the omicron variant in Australia. PLoS Genetics. 2022;18(10):e1010415.

52. Zhang C, Stadler T, Klopfstein S, Heath TA, Ronquist F. Total-evidence dating under the fossilized birth–death process. Systematic biology. 2016;65(2):228–249.

53. Stadler T, Vaughan TG, Gavryushkin A, Guindon S, Kühnert D, Leventhal GE, et al. How well can the exponential-growth coalescent approximate constant-rate birth–death population dynamics? Proceedings of the Royal Society B: Biological Sciences. 2015;282(1806):20150420.

54. Volz EM, Frost SD. Sampling through time and phylodynamic inference with coalescent and birth–death models. Journal of The Royal Society Interface. 2014;11(101):20140945.

55. Featherstone LA, Di Giallonardo F, Holmes EC, Vaughan TG, Duchêne S. Infectious disease phylodynamics with occurrence data. Methods in Ecology and Evolution. 2021;12(8):1498–1507.

56. Jukes TH, Cantor CR, et al. Evolution of protein molecules. Mammalian protein metabolism. 1969;3(24):21–132.

57. Ho SY, Duchêne S, Duchêne D. Simulating and detecting autocorrelation of molecular evolutionary rates among lineages. Molecular ecology resources. 2015;15(4):688–696.

58. Schliep KP. phangorn: phylogenetic analysis in R. Bioinformatics. 2011;27(4):592–593.